



CHAPTER V

APPLICATION AND RESULTS

In order to demonstrate the accuracy of the proposed method, four cases of boundary conditions for skew plate subjected to uniformly distributed loads have been calculated and compared with the results of other investigators and those of the acceptable finite element program "sap⁴". The computer program has been developed in "fortran 77" language for any skew plate angles and aspect ratios with the poisson's ratio of 0.3. All of the programs and numerical results have included in appendix C and D respectively.

Example 1 : All Edges are Simply-Supported

The sets of boundary integral equation (36) and (37) are employed for calculating the normal slope and equivalent shear force on the boundaries. The deflections and stress resultants in domain can be found from equation (75) and its appropriate differentiating.

$$w(\xi, \eta) = \sum_{j=1}^n N_j[X_1, X_2] \int_{\Gamma_j} \bar{M}[X_1, X_2; \xi, \eta] d\Gamma_j[X_1, X_2]$$

$$+ \sum_{j=1}^n V_j[X_1, X_2] \int_{\Gamma_j} \bar{W}[X_1, X_2; \xi, \eta] d\Gamma_j[X_1, X_2]$$

$$\begin{aligned}
 & n+4 \\
 & + \sum_{j=n+1}^{n+4} R_j[X_1, X_2] \dot{W}_j^*[X_1, X_2; \xi, \eta] \\
 & j = n+1 \\
 & + \int_{\Omega} q \dot{W}^*[X_1, X_2; \xi, \eta] d\Omega[X_1, X_2] \tag{75}
 \end{aligned}$$

Table 1. provides the central deflections and bending moments for various of aspect ratios with 90° skew angle or rectangular plates and compares the results to those obtained by analytical method as quoted by Timoshenko [7]. The error column in the table indicates the excellent agreement of the results. The variation of deflections and bending moments are plotted in figure 14 through 22 corresponding to 75° , 60° and 45° skew angles with aspect ratio = 1, and compares to those obtained by finite element (sap⁴). In each case the BEM results refer to 40 boundary elements, which corresponds to 256 elements in the finite element method. These figures shows close agreement of all variables calculated.

Example II : All Edges are Clamped

The sets of boundary integral equations (38) and (39) are employed for calculating the bending moments and equivalent shear on the boundaries. The deflections and stress resultants in domain can be found from equation (76) and its appropriate differentiating.

$$\begin{aligned}
 & n \\
 W(\xi, \eta) = & \sum_{j=1}^n M_j[X_1, X_2] \int_{\Gamma_j} \dot{N}^*[X_1, X_2; \xi, \eta] d\Gamma_j[X_1, X_2] \\
 & j = 1
 \end{aligned}$$

$$\begin{aligned}
& + \sum_{j=1}^n V_j[X_1, X_2] \int_{\Gamma_j} \bar{W}[X_1, X_2; \xi, \eta] d\Gamma_j[X_1, X_2] \\
& + \sum_{j=n+1}^{n+4} R_j[X_1, X_2] \bar{W}_j[X_1, X_2; \xi, \eta] \\
& + \int_{\Omega} q \bar{W}[X_1, X_2; \xi, \eta] d\Omega[X_1, X_2] \tag{76}
\end{aligned}$$

The results are recorded in table 2 and plotted in figure 23 through 31 and compared to the results that quoted by Timoshenko [7] and finite element methods respectively. All of the results show the good agreement .

Example III : Two Opposite Edges Simply-Supported and the Other Two Edges Clamped

In the case of mixed boundary conditions , it will be better to separate the boundaries by its boundary conditions as follow :

Γ_1 = first side [clamped] :

$$[W] = [N] = 0 \quad ; \quad j = 1, 2, \dots, n_1$$

Γ_2 = second side [simply-supported] :

$$[W] = [M] = 0 \quad ; \quad j = n_1+1, n_1+2, \dots, n_2$$

Γ_3 = thirde side [clamped] :

$$[W] = [N] = 0 \quad ; \quad j = n_2+1, n_2+2, \dots, n_3$$

Γ_4 = fourth side [simply-supported] :

$$[W] = [M] = 0 \quad ; \quad j = n_3+1, n_3+2, \dots, n$$

$$\Gamma = \Gamma_1 + \Gamma_2 + \Gamma_3 + \Gamma_4$$

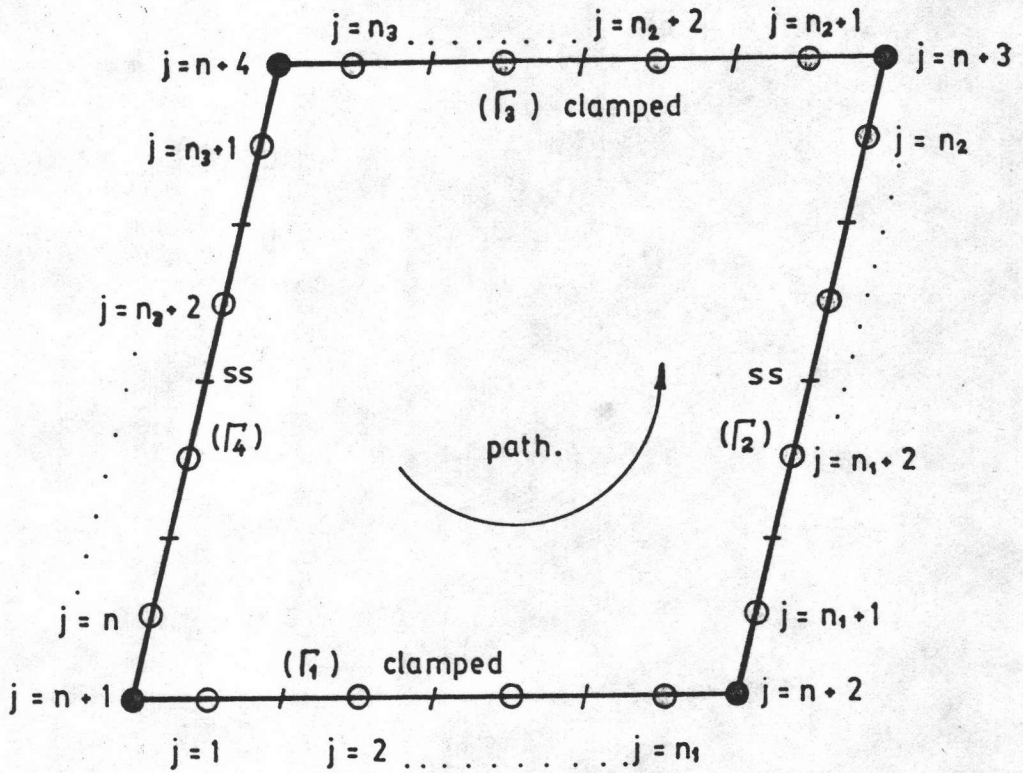


FIG.12 Boundary Discretization

Substitute these boundary conditions in to equation (31) ,
 (32) and (33) yields :

$$W(\xi, \eta) = - \sum_{j=1}^{n_1} M_j[X_1, X_2] \int_{\Gamma_j} N^*[X_1, X_2; \xi, \eta] d\Gamma_j[X_1, X_2]$$

$$+ \sum_{j=n_1+1}^{n_2} N_j[X_1, X_2] \int_{r_j} \overset{*}{M}[X_1, X_2; \xi, \eta] d\Gamma_j[X_1, X_2]$$

$$j = n_1 + 1$$

$$- \sum_{j=n_2+1}^{n_3} M_j[X_1, X_2] \int_{r_j} \overset{*}{N}[X_1, X_2; \xi, \eta] d\Gamma_j[X_1, X_2]$$

$$j = n_2 + 1$$

$$+ \sum_{j=n_3+1}^n N_j[X_1, X_2] \int_{r_j} \overset{*}{M}[X_1, X_2; \xi, \eta] d\Gamma_j[X_1, X_2]$$

$$j = n_3 + 1$$

$$+ \sum_{j=1}^n V_j[X_1, X_2] \int_{r_j} \overset{*}{W}[X_1, X_2; \xi, \eta] d\Gamma_j[X_1, X_2]$$

$$j = 1$$

$$+ \sum_{j=n+1}^{n+4} R_j[X_1, X_2] \overset{*}{W}_j[X_1, X_2; \xi, \eta]$$

$$j = n + 1$$

$$+ \int_{\Omega} \overset{*}{W}[X_1, X_2; \xi, \eta] d\Omega[X_1, X_2] \quad (77)$$

$$Y W(\overset{*}{\xi}_1, \overset{*}{\eta}_1) = - \sum_{j=1}^{n_1} M_j[X_1, X_2] \int_{r_j} \overset{*}{N}[X_1, X_2; \overset{*}{\xi}_1, \overset{*}{\eta}_1] d\Gamma_j[X_1, X_2]$$

$$2\pi \quad j = 1$$

$$\begin{aligned}
 & + \sum_{j=n_1+1}^{n_2} N_j[X_1, X_2] \int_{\Gamma_j} \overset{*}{M}[X_1, X_2; \bar{\xi}_1, \bar{\eta}_1] d\Gamma_j[X_1, X_2] \\
 & j = n_1 + 1
 \end{aligned}$$

$$\begin{aligned}
 & - \sum_{j=n_2+1}^{n_3} M_j[X_1, X_2] \int_{\Gamma_j} \overset{*}{N}[X_1, X_2; \bar{\xi}_1, \bar{\eta}_1] d\Gamma_j[X_1, X_2] \\
 & j = n_2 + 1
 \end{aligned}$$

$$\begin{aligned}
 & + \sum_{j=n_3+1}^n N_j[X_1, X_2] \int_{\Gamma_j} \overset{*}{M}[X_1, X_2; \bar{\xi}_1, \bar{\eta}_1] d\Gamma_j[X_1, X_2] \\
 & j = n_3 + 1
 \end{aligned}$$

$$\begin{aligned}
 & + \sum_{j=1}^n V_j[X_1, X_2] \int_{\Gamma_j} \overset{*}{W}[X_1, X_2; \bar{\xi}_1, \bar{\eta}_1] d\Gamma_j[X_1, X_2] \\
 & j = 1
 \end{aligned}$$

$$\begin{aligned}
 & + \sum_{j=n+1}^{n+4} R_j[X_1, X_2] \overset{*}{W}_j[X_1, X_2; \bar{\xi}_1, \bar{\eta}_1] \\
 & j = n + 1
 \end{aligned}$$

$$+ \int_{\Omega} q \overset{*}{W}[X_1, X_2; \bar{\xi}_1, \bar{\eta}_1] d\Omega[X_1, X_2] \quad ; \quad i = 1, 2, \dots, n+4 \quad (78)$$

$$\frac{1}{2\pi} N(\bar{\xi}_1, \bar{\eta}_1) = - \sum_{j=1}^{n_1} \frac{M_j[X_1, X_2] \int_{\Gamma_j} \overset{*}{N}[X_1, X_2; \bar{\xi}_1, \bar{\eta}_1] d\Gamma_j[X_1, X_2]}{\partial n[\bar{\xi}, \bar{\eta}]}$$

$$+ \sum_{j = n_1 + 1}^{n_2} N_j [X_1, X_2] \int_{\Gamma_j} \frac{\partial M^* [X_1, X_2; \bar{\xi}_1, \bar{\eta}_1] d\Gamma_j [X_1, X_2]}{\partial n [\bar{\xi}, \bar{\eta}]}$$

$$- \sum_{j = n_2 + 1}^{n_3} M_j [X_1, X_2] \int_{\Gamma_j} \frac{\partial N^* [X_1, X_2; \bar{\xi}_1, \bar{\eta}_1] d\Gamma_j [X_1, X_2]}{\partial n [\bar{\xi}, \bar{\eta}]}$$

$$+ \sum_{j = n_3 + 1}^n N_j [X_1, X_2] \int_{\Gamma_j} \frac{\partial M^* [X_1, X_2; \bar{\xi}_1, \bar{\eta}_1] d\Gamma_j [X_1, X_2]}{\partial n [\bar{\xi}, \bar{\eta}]}$$

$$+ \sum_{j = 1}^n V_j [X_1, X_2] \int_{\Gamma_j} \frac{\partial W^* [X_1, X_2; \bar{\xi}_1, \bar{\eta}_1] d\Gamma_j [X_1, X_2]}{\partial n [\bar{\xi}, \bar{\eta}]}$$

$$+ \sum_{j = n+1}^{n+4} R_j [X_1, X_2] \frac{\partial \bar{W}_j^* [X_1, X_2; \bar{\xi}_1, \bar{\eta}_1]}{\partial n [\bar{\xi}, \bar{\eta}]}$$

$$+ \int_a^q \frac{\partial W^* [X_1, X_2; \bar{\xi}_1, \bar{\eta}_1] d\Omega [X_1, X_2]}{\partial n [\bar{\xi}, \bar{\eta}]} \quad ; \quad i = 1, 2, \dots, n \quad (79)$$

Equations (78) and (79) can be expressed in matrix form as follows :

$$\begin{bmatrix} [N]_{r1} & -[M]_{r2} & [N]_{r3} & -[M]_{r4} & -[W]_r & -[W_c]_r \\ [N]_{r1} & -[M]_{r2} & [N]_{r3} & -[M]_{r4} & -[W]_r & -[W_c]_r \end{bmatrix} \begin{bmatrix} [M]_{r1} \\ [N]_{r2} \\ [M]_{r3} \\ [N]_{r4} \\ [V]_r \\ [R] \end{bmatrix} = \begin{bmatrix} [Q] \\ [Q] \\ [Q] \\ [Q] \\ [Q] \\ [Q] \end{bmatrix} \quad (80)$$

The boundary function can be calculated from equation (80) by " Gauss Elimination Method " [11]. Therefore , deflections and stress resultants can be found from equation (78) and its appropriate differentiating.

The numerical results are recorded in table 3 and plotted in figure 32 through 40 which show excellent agreement with the results quoted by Timoshenko [7] and those obtained by finite element method respectively.

Example IV Two Opposite Edges Simply-Supported and the Other Two Edges Free

By the same procedure as shown in example III , the sets of boundary integral equations can be expressed in equation (81) and domain integral equation in (82).

$$\begin{aligned}
 & n_2 \\
 & + \sum_{j=n_1+1}^{n_2} V_j[X_1, X_2] \int_{\Gamma_j} \bar{W}[X_1, X_2; \xi, \eta] d\Gamma_j[X_1, X_2] \\
 & j = n_1 + 1
 \end{aligned}$$

$$\begin{aligned}
 & n_3 \\
 & - \sum_{j=n_2+1}^{n_3} W_j[X_1, X_2] \int_{\Gamma_j} \bar{V}[X_1, X_2; \xi, \eta] d\Gamma_j[X_1, X_2] \\
 & j = n_2 + 1
 \end{aligned}$$

$$\begin{aligned}
 & n \\
 & + \sum_{j=n_3+1}^n V_j[X_1, X_2] \int_{\Gamma_j} \bar{W}[X_1, X_2; \xi, \eta] d\Gamma_j[X_1, X_2] \\
 & j = n_3 + 1
 \end{aligned}$$

$$\begin{aligned}
 & n \\
 & + \sum_{j=1}^n N_j[X_1, X_2] \int_{\Gamma_j} \bar{M}[X_1, X_2; \xi, \eta] d\Gamma_j[X_1, X_2] \\
 & j = 1
 \end{aligned}$$

$$\begin{aligned}
 & n+4 \\
 & + \sum_{j=n+1}^{n+4} R_j[X_1, X_2] \bar{W}_j[X_1, X_2; \xi, \eta] \\
 & j = n+1
 \end{aligned}$$

$$+ \int_{\Omega} q \bar{W}[X_1, X_2; \xi, \eta] d\Omega[X_1, X_2] \quad (82)$$

Table 4 provides the central deflections and bending moments calculated by 20, 40 and 60 boundary elements. These results are in very good agreement with the results quoted by Timoshenko [7], but its convergence is poorer than other examples. Other values of deflections and bending moment distributions have also been computed

as shown in figure 41 through 49. The present deflections and bending moments results are almost coincident with the results of the finite element method except for the moment near the corner and boundary which show some fluctuation and keep increasing instead of vanishing.